2024 IEEE 63rd Conference on Decision and Control (CDC)
December 16-19, 2024. MiCo, Milan, Italy

Towards integrated tracking fault-tolerant control for Takagi-Sugeno systems

Marcin Witczak and Marcin Pazera

Abstract— **This paper addresses the challenge of combining fault estimation and fault-tolerant control for constrained non-linear systems subject to bounded external disturbances. To handle the nonlinearities, the fuzzy Takagi-Sugeno (T-S) methodology is utilised. As a consequence, gains of the estimator and controller are calculated for all the vertices of the polytopic set. Specifically, the intertwined nature of control and estimation leads to mutual influence, necessitating a novel integration approach to avoid deteriorating the overall system performance. A new strategy is introduced, grounded on a critical existence condition that is both necessary and sufficient. The suggested method operates through output feedback and unfolds in two distinct phases: the *off-line* phase involves a straightforward optimization task utilizing the set of Linear Matrix Inequalities (LMIs), while the *on-line* phase tackles a deterministic model predictive control issue.**

I. Introduction

Owing to the intense development of Industrial Internet of Things (IIoT) [19] towards Industry 4.0, companies are increasing the number of sensors and actuators that cover the existing and newly developed infrastructures. The pursuit of advancements in fault detection and fault-tolerant control mechanisms forms a cornerstone of contemporary control system research and application. A particularly innovative approach is the integration of output feedback-based fault-tolerant control systems, initially put forth for deterministic systems characterized by linear and Takagi-Sugeno (T-S) frameworks [17]. This concept has since been adapted to accommodate systems defined by linear parameter variations and those exhibiting Lipschitz continuity [3], [18], extending even to non-deterministic linear system models [11] as well as T-S [10] and LPV [4] systems.

However, the interplay between fault estimation (FE) and fault-tolerant control (FTC) [5], [7] introduces a bidirectional influence that complicates their integration, leading to potential degradation in system performance. To address this, previous studies have presented strategies that rely on a unified optimization problem formulated through linear matrix inequalities (LMIs) [9], [10]. Despite the theoretical appeal of these methods, they are often criticized for the complexity and computational demands associated with the LMI formulations, particularly when applied to complex system models.

Recent research involving FTC includes e.g. a switched state and fault estimation along with FTC for T-S fuzzy systems [8], in which an observer has been created for the dual purpose of estimating the system states and identifying both sensor and actuator faults, despite the presence of sensor fault-affected measurement outputs. Utilizing this observer as a foundation, a switched fuzzy FTC strategy is formulated to ensure the stability of the closed-loop system while mitigating the impacts of various faults under consideration, all the while acknowledging external disturbances. The symbiotic relationship between the estimation unit and the control unit facilitates a cohesive design approach for these units, contrasting with a disjointed design methodology. In [16] the authors consider a finite-time fault-tolerant trajectory tracking control for a quadrotor. In such a work a Sliding Mode Control (SMC) is proposed to separately accommodate the parametric uncertainties and actuator faults. In [20] a switched LPV approach in discrete-time domain is utilized for achieving an active FTC, where both input and output matrices can be of parameter-dependent form. A proposed in [15] approach guarantees the precision and optimality of fault estimation by actively designing optimal inputs at each time instant under the set-theoretic framework.

In light of these challenges, this paper presents a novel approach that aims to refine the integration of FE and FTC. By adopting a quadratic robustness strategy [1], our work introduces a simpler, yet effective, methodology that reduces the computational burden while enhancing the system's ability to manage faults under input and output constraints. The proposed method unfolds in two distinct phases: an offline optimization phase that establishes a low-complexity LMI framework [14], and an online phase that utilizes deterministic model predictive control [2], [6]. This bifurcated approach not only addresses the bidirectional interference between FE and FTC but also ensures the system's adherence to predefined performance metrics even in the presence of faults and external disturbances. The overall scheme of the utilized appraoch can be presented as the one in Fig. 1.

The paper is organized as follows: Section II formulates a problem for a proposed system considered in Takagi-Sugeno (T-S) fuzzy form. In Sec. III an integrated FTC design algorithm is presented along with stability considerations, while Sec. IV provides a two-phase design methodology approach. Subsequently, Sec. V presents an illustrative example with application to a two-tank system, and finally, Sec. VI concludes the paper.

II. Problem formulation

Consider the system outlined below

$$\boldsymbol{x}_{k+1} = \boldsymbol{f}\left(\boldsymbol{x}_k, \boldsymbol{u}_k\right), \tag{1}$$

M. Witczak and M. Pazera are with the Institute of Control and Computation Engineering, University of Zielona Gora, ul. Szafrana 2, 65-516 Zielona Gora, Poland (e-mail: {m.witczak,m.pazera}@issi.uz.zgora.pl).

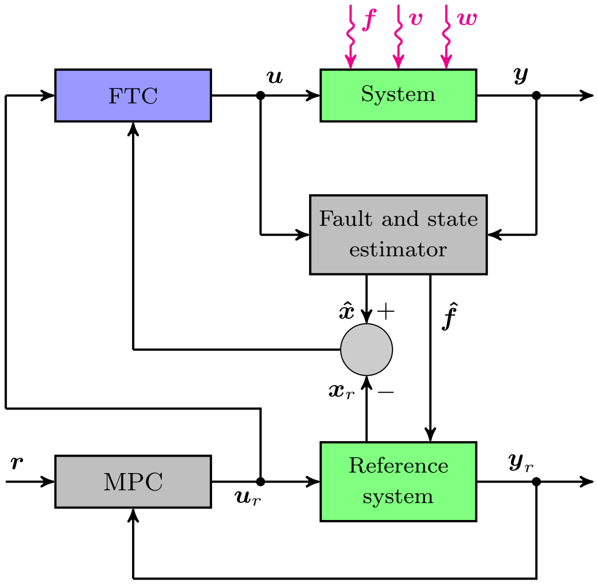

Fig. 1. A scheme of the proposed approach.

which is aptly represented using a Takagi-Sugeno (T-S) framework that incorporates both faults and uncertainties:

$$\begin{aligned}\boldsymbol{x}_{k+1} &= \boldsymbol{A}\left(\boldsymbol{p}_k\right)\boldsymbol{x}_k + \boldsymbol{B}\left(\boldsymbol{p}_k\right)\boldsymbol{u}_k + \boldsymbol{B}\left(\boldsymbol{p}_k\right)\boldsymbol{f}_k + \boldsymbol{W}\boldsymbol{w}_k \\ &= \sum_{i=1}^{M}\boldsymbol{h}_i\left(\boldsymbol{p}_k\right)\left[\boldsymbol{A}^i\boldsymbol{x}_k + \boldsymbol{B}^i\boldsymbol{u}_k + \boldsymbol{B}^i\boldsymbol{f}_k\right] + \boldsymbol{W}\boldsymbol{w}_k,\end{aligned} \tag{2}$$

$$\boldsymbol{y}_k = \boldsymbol{C}\boldsymbol{x}_k + \boldsymbol{V}\boldsymbol{v}_k, \tag{3}$$

accompanied by

$$\boldsymbol{h}_i\left(\boldsymbol{p}_k\right) \geq 0 \quad \forall i = 1,\ldots,M \qquad \sum_{i=1}^{M}\boldsymbol{h}_i\left(\boldsymbol{p}_k\right) = 1, \tag{4}$$

where the variables $x_k \in X \subseteq \mathbb{R}^{n_x}$ and $u_k \in U \subseteq \mathbb{R}^{n_u}$ represent the restricted state and control input respectively, under the conditions:

$$\mathbb{X} = \{\boldsymbol{x} : \underline{x}_i \leq x_{i,k} \leq \bar{x}_i, \quad i = 1,\ldots,n_x\}, \tag{5}$$

$$\mathbb{U} = \{\boldsymbol{u} : \underline{u}_j \leq u_{j,k} \leq \bar{u}_j, \quad j = 1,\ldots,n_u\}, \tag{6}$$

with $\underline{x}_i < \bar{x}_i$ and $\underline{u}_j < \bar{u}_j$. Furthermore, $\boldsymbol{f}_k \in F_a \subseteq \mathbb{R}^r$ signifies the actuator defect. The potential evolution of this defect is limited to an ellipsoid $\boldsymbol{e}_k = \boldsymbol{f}_{k+1} - \boldsymbol{f}_k \in \mathbb{E}\epsilon$. Additionally, $\boldsymbol{w}_k \in \mathbb{E}_w$ and $\boldsymbol{v}_k \in \mathbb{E}_v$ are ellipsoidally constrained exogenous disturbances. The matrices $\boldsymbol{B}\left(\boldsymbol{p}_k\right)$, $\boldsymbol{C}$ are assumed to have full rank and it is given that $n_u \leq n_y$. This indicates a limitation on estimating more faults than the number of measured outputs. Additionally, $\boldsymbol{h}_i(\cdot)$ symbolizes the strength of rule firing as defined by Takagi and Sugeno, based on the measurable premise variables vector $\boldsymbol{p}_k = \left[\boldsymbol{p}_k^1, \boldsymbol{p}_k^2, \ldots, \boldsymbol{p}_k^p\right]^T$.

The input to the potentially defective system as described by equations (2)-(3) must be configured to enable $\boldsymbol{x}_k$ to follow the target state $\boldsymbol{x}_{r,k}$, which is governed by:

$$\boldsymbol{x}_{r,k+1} = \boldsymbol{A}\left(\boldsymbol{p}_k\right)\boldsymbol{x}_{r,k} + \boldsymbol{B}\left(\boldsymbol{p}_k\right)\boldsymbol{u}_{r,k} + \boldsymbol{B}\left(\boldsymbol{p}_k\right)\hat{\boldsymbol{f}}_k, \tag{7}$$

$$\boldsymbol{y}_{r,k} = \boldsymbol{C}\boldsymbol{x}_{r,k}, \tag{8}$$

$$\boldsymbol{z}_{r,k} = \boldsymbol{H}\boldsymbol{x}_{r,k}, \tag{9}$$

where $\boldsymbol{z}_{r,k} \in \mathbb{Z}^{n_z}$ with $n_z \leq n_u$. The dimensions of these variables match those in (2)-(3). Moreover, the system defined by equations (7)-(9) should track the reference $\boldsymbol{r}_k$, aiming for $\boldsymbol{z}_k$ to converge towards $\boldsymbol{r}_k$. The reference $\boldsymbol{r}_k$ is known over a limited preview horizon n_h, meaning $\boldsymbol{r}_k, \ldots, r_{k+n_h-1}$ are available. Unlike existing methodologies cited in the literature, the reference system involving the fault estimate may affect its capacity to achieve $\boldsymbol{r}_k$. The advantage here lies in the ability to assess control feasibility at the level of the reference system rather than the faulty one, allowing for possible adjustments to $\boldsymbol{r}_k$. Now, we define a state and fault estimator to approximate $\hat{\boldsymbol{x}}_k$ and $\hat{\boldsymbol{f}}_k$ as follows:

$$\begin{aligned}\hat{\boldsymbol{x}}_{k+1} = \boldsymbol{A}\left(\boldsymbol{p}_k\right)\hat{\boldsymbol{x}}_k + \boldsymbol{B}\left(\boldsymbol{p}_k\right)\boldsymbol{u}_k + \boldsymbol{B}\left(\boldsymbol{p}_k\right)\hat{\boldsymbol{f}}_k \\ + \boldsymbol{K}\left(\boldsymbol{y}_k - \boldsymbol{C}\hat{\boldsymbol{x}}_k\right),\end{aligned} \tag{10}$$

$$\hat{\boldsymbol{f}}_{k+1} = \hat{\boldsymbol{f}}_k + \boldsymbol{F}\left(\boldsymbol{y}_k - \boldsymbol{C}\hat{\boldsymbol{x}}_k\right), \tag{11}$$

where $\boldsymbol{K}$ and $\boldsymbol{F}$ are the gain matrices of the estimator. The integrated control strategy is represented by:

$$\boldsymbol{u}_k = -\boldsymbol{K}_c(\hat{\boldsymbol{x}}_k - \boldsymbol{x}_{r,k}) + \boldsymbol{u}_{r,k}, \tag{12}$$

The primary challenge involves accommodating the unknown effect of $\boldsymbol{f}_k$, considering the limited actuator performance as outlined. This approach diverges from those found in existing studies by avoiding conservative assumptions about compensating for an actuator fault with the same defective actuator. Instead, a strategic control allocation among available actuators ensures efficient fault management. To further our discussion, let's define performance measures as state and actuator fault errors ($\boldsymbol{e}_k = \boldsymbol{x}_k - \hat{\boldsymbol{x}}_k$, $\boldsymbol{e}_{f,k} = \boldsymbol{f}_k - \hat{\boldsymbol{f}}_k$) and tracking and reference errors ($\boldsymbol{e}_{t,k} = \hat{\boldsymbol{x}}_k - \boldsymbol{x}_{r,k}$, $\boldsymbol{e}_{r,k} = \boldsymbol{x}_k - \boldsymbol{x}_{r,k}$), with a relationship established through $\boldsymbol{e}_{t,k} = \boldsymbol{e}_{r,k} - \boldsymbol{e}_k$. Hence, substituting equations (2)-(3), (7)-(8), and (12), we derive the dynamics of these errors:

$$\begin{aligned}\boldsymbol{e}_{r,k+1} = (\boldsymbol{A}\left(\boldsymbol{p}_k\right) - \boldsymbol{B}\left(\boldsymbol{p}_k\right)\boldsymbol{K}_c)\boldsymbol{e}_{r,k} \\ + \boldsymbol{B}\left(\boldsymbol{p}_k\right)\boldsymbol{K}_c\boldsymbol{e}_k + \boldsymbol{B}\left(\boldsymbol{p}_k\right)\boldsymbol{e}_{f,k} + \boldsymbol{W}\boldsymbol{w}_k,\end{aligned} \tag{13}$$

$$\begin{aligned}\boldsymbol{e}_{t,k+1} = (\boldsymbol{A}\left(\boldsymbol{p}_k\right) - \boldsymbol{B}\left(\boldsymbol{p}_k\right)\boldsymbol{K}_c)\boldsymbol{e}_{t,k} \\ - \boldsymbol{K}(\boldsymbol{y}_k - \boldsymbol{C}\hat{\boldsymbol{x}}_k),\end{aligned} \tag{14}$$

$$\begin{aligned}\boldsymbol{e}_{k+1} = (\boldsymbol{A}\left(\boldsymbol{p}_k\right) - \boldsymbol{K}\boldsymbol{C})\boldsymbol{e}_k + \boldsymbol{B}\left(\boldsymbol{p}_k\right)\boldsymbol{e}_{f,k} + \boldsymbol{W}\boldsymbol{w}_k \\ - \boldsymbol{K}\boldsymbol{V}\boldsymbol{v}_k,\end{aligned} \tag{15}$$

$$\boldsymbol{e}_{f,k+1} = \boldsymbol{e}_{f,k} - \boldsymbol{F}\boldsymbol{C}\boldsymbol{e}_k - \boldsymbol{F}\boldsymbol{V}\boldsymbol{v}_k + \boldsymbol{\varepsilon}_k. \tag{16}$$

It is noted that $\boldsymbol{e}_{t,k}$ can be directly calculated, containing both $\boldsymbol{B}\left(\boldsymbol{p}_k\right)\boldsymbol{K}_c$ and $\boldsymbol{K}\boldsymbol{C}$ terms known for computational difficulties, whereas $\boldsymbol{e}_{r,k}$, though not directly computable, only includes the $\boldsymbol{B}\boldsymbol{K}_c$ term. The goal of the next section is to suggest an integrated and simultaneous design of the control input based on equations (13), (15), and (16).

III. Integrated FTC design

As outlined in the study by [12], crafting an estimator and controller to operate in tandem poses a significant challenge. The work by [12] introduces a proximate solution to address this issue. This section introduces an approach that is less restrictive. Before diving into the specifics, let's recast (13) along with (15)–(16) into the framework of (18)

$$\begin{aligned} \boldsymbol{e}_{r,k+1} &= (\boldsymbol{A}(\boldsymbol{p}_k) - \boldsymbol{B}(\boldsymbol{p}_k)\boldsymbol{K}_c)\boldsymbol{e}_{r,k} \\ &\quad + [\boldsymbol{B}(\boldsymbol{p}_k)\boldsymbol{K}_c, , [\boldsymbol{B}(\boldsymbol{p}_k), \boldsymbol{W}]]\tilde{\boldsymbol{w}}_k, \end{aligned} \tag{17}$$

where $\tilde{\boldsymbol{w}}_k = [\bar{\boldsymbol{e}}_k^T, \boldsymbol{w}_k^T]^T$ and $\bar{\boldsymbol{e}}_k = [\boldsymbol{e}_k^T, \boldsymbol{e}_{f,k}^T]^T$ are confined within an ellipsoidal bound $\mathbb{E}\tilde{\boldsymbol{w}}, \boldsymbol{Q}_c$, with $\boldsymbol{Q}_c = \frac{1}{2}\text{diag}(\boldsymbol{P}_e, \boldsymbol{Q}_w)$. It's important to recognize that the estimation error is considered to be within the bounds of $\mathbb{E}\bar{\boldsymbol{e}}, \boldsymbol{P}_e$, and the method for determining $\boldsymbol{P}_e \succ \boldsymbol{0}$ will be discussed subsequently. The transformation of (15)–(16) into the format of

$$\boldsymbol{z}_{k+1} = \boldsymbol{A}(\boldsymbol{p}_k)\boldsymbol{z}_k + [\boldsymbol{G}\,\boldsymbol{B}(\boldsymbol{p}_k)]\boldsymbol{w}_k \tag{18}$$

proceeds as follows:

$$\bar{\boldsymbol{e}}_{k+1} = (\bar{\boldsymbol{A}}(\boldsymbol{p}_k) - \bar{\boldsymbol{K}}\bar{\boldsymbol{C}})\bar{\boldsymbol{e}}_k + [-\bar{\boldsymbol{K}}\boldsymbol{V}, [\bar{\boldsymbol{W}}, \bar{\boldsymbol{I}}]]\tilde{\boldsymbol{v}}_k, \tag{19}$$

where

$$\bar{\boldsymbol{A}}(\boldsymbol{p}_k) = \begin{bmatrix} \boldsymbol{A}(\boldsymbol{p}_k) & \boldsymbol{B}(\boldsymbol{p}_k) \\ \boldsymbol{0} & \boldsymbol{I} \end{bmatrix}, \bar{\boldsymbol{K}} = \begin{bmatrix} \boldsymbol{K} \\ \boldsymbol{F} \end{bmatrix},$$
$$\bar{\boldsymbol{C}} = [\boldsymbol{C}, \boldsymbol{0}], \qquad \bar{\boldsymbol{W}} = \begin{bmatrix} \boldsymbol{W} \\ \boldsymbol{0} \end{bmatrix}$$

and $\bar{\boldsymbol{I}} = [\boldsymbol{0}, \boldsymbol{I}]^T$, $\tilde{\boldsymbol{v}}_k = [\boldsymbol{v}_k^T, \boldsymbol{w}_k^T, \boldsymbol{\varepsilon}_k^T]^T$, which is bounded within $\mathbb{E}_{\bar{\boldsymbol{e}}, \boldsymbol{Q}_e}$, $\boldsymbol{Q}_e = \frac{1}{3}\text{diag}(\boldsymbol{Q}_v, \boldsymbol{Q}_w, \boldsymbol{Q}_\varepsilon)$. A widely recognized method described in previous studies [9], [10] involves consolidating $\boldsymbol{e}_{r,k}$ and $\bar{\boldsymbol{e}}_k$ into a singular vector, followed by a demonstration of the system's overall convergence. This paper aims to offer a different approach. The principal contribution of this section is encapsulated in the subsequent theorem:

***Theorem** 1:* The systems (17) and (19) are strictly quadratically bounded for all allowable $\tilde{\boldsymbol{w}}_k \in \mathbb{E}_{\tilde{\boldsymbol{w}}, \boldsymbol{Q}_c}$ $\tilde{\boldsymbol{v}}_k \in \mathbb{E}_{\tilde{\boldsymbol{w}}, \boldsymbol{Q}_e}$ iff there exists $\alpha_c \in (0,1)$, $\alpha_e \in (0,1)$, $\boldsymbol{P}_c \succ \boldsymbol{0}$, $\boldsymbol{P}_e \succ \boldsymbol{0}$, $\boldsymbol{U}_c$, $\boldsymbol{U}_e$, $\boldsymbol{N}_c$ and $\boldsymbol{N}_e$:

$$\begin{bmatrix} -(1-\alpha_e)\boldsymbol{P}_e & \boldsymbol{0} & \boldsymbol{0} & \boldsymbol{X}_e^T \\ \boldsymbol{0} & -\alpha_e\boldsymbol{Q}_e^{1,1} & -\alpha_e\boldsymbol{Q}_e^{1,2} & \boldsymbol{Y}_e^T \\ \boldsymbol{0} & -\alpha_e\boldsymbol{Q}_e^{2,1} & -\alpha_e\boldsymbol{Q}_e^{2,2} & \boldsymbol{Z}_e^T \\ \boldsymbol{X}_e(\boldsymbol{p}_k) & \boldsymbol{Y}_e(\boldsymbol{p}_k) & \boldsymbol{Z}_e(\boldsymbol{p}_k) & \boldsymbol{P}_e - \boldsymbol{U}_e^T - \boldsymbol{U}_e \end{bmatrix} \prec \boldsymbol{0}, \tag{20}$$

$\boldsymbol{X}_e(\boldsymbol{p}_k) = \boldsymbol{U}_e\bar{\boldsymbol{A}}(\boldsymbol{p}_k) - \boldsymbol{N}_e\bar{\boldsymbol{C}}, \boldsymbol{Y}_e = -\boldsymbol{N}_e\boldsymbol{V},$
$\boldsymbol{N}_e = \boldsymbol{U}_e\bar{\boldsymbol{K}}, \boldsymbol{Z}_e = [\bar{\boldsymbol{W}}, \bar{\boldsymbol{I}}],$

$$\begin{bmatrix} -(1-\alpha_c)\boldsymbol{P}_c & \boldsymbol{0} & \boldsymbol{0} & \boldsymbol{X}_c^T \\ \boldsymbol{0} & -\alpha_c\boldsymbol{Q}_c^{1,1} & -\alpha_c\boldsymbol{Q}_c^{1,2} & \boldsymbol{Y}_c^T \\ \boldsymbol{0} & -\alpha_c\boldsymbol{Q}_c^{2,1} & -\alpha_c\boldsymbol{Q}_c^{2,2} & \boldsymbol{Z}_c^T \\ \boldsymbol{X}_c(\boldsymbol{p}_k) & \boldsymbol{Y}_c(\boldsymbol{p}_k) & \boldsymbol{Z}_c(\boldsymbol{p}_k) & \boldsymbol{P}_c - \boldsymbol{U}_c^T - \boldsymbol{U}_c \end{bmatrix} \prec \boldsymbol{0} \tag{21}$$

$\boldsymbol{X}_c(\boldsymbol{p}_k) = \boldsymbol{A}(\boldsymbol{p}_k)\boldsymbol{U}_c - \boldsymbol{B}(\boldsymbol{p}_k)\boldsymbol{N}_c, \boldsymbol{Y}_c(\boldsymbol{p}_k) = \boldsymbol{B}(\boldsymbol{p}_k)\boldsymbol{N}_c,$
$\boldsymbol{N}_c = \boldsymbol{K}_c\boldsymbol{U}_c, \boldsymbol{Z}_c(\boldsymbol{p}_k) = [\boldsymbol{B}(\boldsymbol{p}_k), \boldsymbol{W}].$

Proof: We recall the following Lemmas for context:

***Lemma** 1:* The following statements are equivalent:

(i) The system (18) is strictly quadratically bounded with the Lyapunov function V_k for all all allowable $\boldsymbol{w}_k \in \mathbb{E}_w$.

(ii) There exist $\boldsymbol{P}_c \succ 0$, $\boldsymbol{U}_c$, $\text{rank}(\boldsymbol{U}_c) = n_z$, $\alpha_c \in (0,1)$ such that

$$\begin{bmatrix} -(1-\alpha_c)\boldsymbol{P}_c & \boldsymbol{0} & \boldsymbol{U}_c^T\boldsymbol{A}(\boldsymbol{p}_k)^T \\ \boldsymbol{0} & -\alpha_c\boldsymbol{Q}_w & \begin{bmatrix} \boldsymbol{U}_c^T\boldsymbol{G}^T \\ \boldsymbol{B}(\boldsymbol{p}_k)^T \end{bmatrix} \\ \boldsymbol{A}(\boldsymbol{p}_k)_c\boldsymbol{U}_c & [\boldsymbol{G}\boldsymbol{U}_c \quad \boldsymbol{B}(\boldsymbol{p}_k)] & \boldsymbol{P}_c - \boldsymbol{U}_c^T - \boldsymbol{U}_c \end{bmatrix} \prec \boldsymbol{0} \tag{22}$$

(iii) There exist $\boldsymbol{P}_e \succ 0$, $\boldsymbol{U}_e$, $\text{rank}(\boldsymbol{U}_e) = n_z$, $\alpha_e \in (0,1)$ such that

$$\begin{bmatrix} -(1-\alpha_e)\boldsymbol{P}_e & \boldsymbol{0} & \boldsymbol{A}(\boldsymbol{p}_k)_e^T\boldsymbol{U}_e^T \\ \boldsymbol{0} & -\alpha_e\boldsymbol{Q}_w & \begin{bmatrix} \boldsymbol{G}_e^T\boldsymbol{U}_e^T \\ \boldsymbol{B}(\boldsymbol{p}_k)^T \end{bmatrix} \\ \boldsymbol{U}_e\boldsymbol{A}(\boldsymbol{p}_k) & [\boldsymbol{U}_e\boldsymbol{G} \quad \boldsymbol{B}(\boldsymbol{p}_k)] & \boldsymbol{P}_e - \boldsymbol{U}_e^T - \boldsymbol{U}_e \end{bmatrix} \prec \boldsymbol{0} \tag{23}$$

***Lemma** 2:* [1] The following statements are equivalent:

(i) The system (18) is strictly quadratically bounded with with the Lyapunov function V_k for all all allowable $\boldsymbol{w}_k \in \mathbb{E}_w$.

(i) The ellipsoid is a positively invariant set for all allowable $\boldsymbol{w}_k \in \mathbb{E}_w$.

(i) There exists $\alpha \in (0,1)$ such that the following inequality is satisfied for all allowable $\boldsymbol{w}_k \in \mathbb{E}_w$:

$$V_{k+1} - (1-\alpha)V_k - \alpha\boldsymbol{w}_k^T\boldsymbol{Q}_w\boldsymbol{w}_k < 0, \tag{24}$$

Let us commence by acknowledging that, according to Lemma 1 (items (i) and (iii)), the fulfillment of (20) is tantamount to (19) being strictly quadratically bounded. Consequently, invoking Lemma 2, the set $\mathbb{E}_{\bar{\boldsymbol{e}}, \boldsymbol{P}_e}$, denoted as $\bar{\boldsymbol{e}}_k^T\boldsymbol{P}_e\bar{\boldsymbol{e}}_k \leq 1$, is established as an invariant set for (19). This also constructs $\boldsymbol{Q}_c = \frac{1}{2}\text{diag}(\boldsymbol{P}_e, \boldsymbol{Q}_w)$, delineating the permissible set for $\tilde{\boldsymbol{w}}_k$ in (17). Following this, Lemma 1 (items (i) and (ii)) postulates that adherence to (21) corresponds to the strict quadratic boundedness of (17). In conclusion, the integrity of $\boldsymbol{U}_e$ and $\boldsymbol{U}_c$ is corroborated by Lemma 1. ■

***Theorem** 2:* If the systems (17) and (19) are strictly quadratically bounded for all all allowable $\boldsymbol{w}_k \in \mathbb{E}_w$ then there exists $\alpha_e \in (0,1)$ and $\alpha_c \in (0,1)$ such that:

$$\lim_{k\to\infty}(1-\alpha_e)^k\|\bar{\boldsymbol{e}}_k\| = 0 \quad \text{for } \tilde{\boldsymbol{w}}_k = \boldsymbol{0}, \tag{25}$$

$$\|\bar{\boldsymbol{e}}_k\|_{l_2}^{\boldsymbol{P}_e} < \|\tilde{\boldsymbol{w}}_k\|_{l_2}^{\boldsymbol{Q}_e} \quad \text{for } \tilde{\boldsymbol{w}}_k \neq \boldsymbol{0}. \tag{26}$$

$$\lim_{k\to\infty}(1-\alpha_c)^k\|\boldsymbol{e}_{r,k}\| = 0 \quad \text{for } \tilde{\boldsymbol{v}}_k = \boldsymbol{0}, \tag{27}$$

$$\|\boldsymbol{e}_{r,k}\|_{l_2}^{\boldsymbol{P}_c} < \|\tilde{\boldsymbol{v}}_k\|_{l_2}^{\boldsymbol{Q}_c} \quad \text{for } \tilde{\boldsymbol{v}}_k \neq \boldsymbol{0}. \tag{28}$$

Proof: The proof follows directly from Theorem 1 and and a following Lemma:

***Lemma** 3:* If the system (18) is strictly quadratically bounded with V_k for all all allowable $\boldsymbol{w}_k \in \mathbb{E}_w$ then there exists $\alpha \in (0,1)$ such that

$$\lim_{k\to\infty}(1-\alpha)^k\|\boldsymbol{z}_k\| = 0 \quad \text{for } \boldsymbol{w}_k = \boldsymbol{0}, \tag{29}$$

$$\|\boldsymbol{z}_k\|_{l_2}^{\boldsymbol{P}} < \|\boldsymbol{w}_k\|_{l_2}^{\boldsymbol{Q}_w} \quad \text{for } \boldsymbol{w}_k \neq \boldsymbol{0}. \tag{30}$$

■

IV. A Two-Phase Design Methodology Approach

A. Phase 1: Off-line Determination of Integrated FTC

We initiate by acknowledging that, given fixed $\alpha_c \in (0,1)$ and $\alpha_e \in (0,1)$, the inequalities (20)–(21) straightforwardly transform into LMIs. This is a direct consequence of Theorem 2 ((25) and (27)), indicating that larger values facilitate faster convergence of the corresponding errors. Conversely, matrices $\boldsymbol{P}_e$ and $\boldsymbol{P}_c$ delineate the ellipsoidal invariant set for these errors, envisioned as regions of uncertainty, which ideally should be minimized. This notion is encapsulated in (26) and (28). Therefore, it is feasible to minimize certain geometrical metrics, such as the volume, which equates to maximizing the determinant of the pertinent matrix, whether $\boldsymbol{P}_e$ or $\boldsymbol{P}_c$. This optimization criterion is denoted as $J(\alpha_c, \alpha_e, \boldsymbol{P}_e, \boldsymbol{P}_c)$. An offline iterative process, comprising the subsequent steps, can be readily executed:

1) Choose $\alpha_c \in (0,1)$ and $\alpha_e \in (0,1)$.
2) Optimize $J(\alpha_c, \alpha_e, \boldsymbol{P}_e, \boldsymbol{P}_c)$ subject to (20)–(21).

This off-line methodology yields the gain matrices for the estimator (10)–(11) and the controller (12) from (20)–(21) as:

$$\bar{\boldsymbol{K}} = \boldsymbol{U}_e^{-1}\boldsymbol{N}_e, \quad \boldsymbol{K}_c = \boldsymbol{N}_c\boldsymbol{U}_c^{-1}. \tag{31}$$

B. Phase II: On-line Determination of Reference Values and FTC

It becomes apparent from (12) and (6) that:

$$\mathbb{U}_{r,k} = \{u_{r,k} : \underline{u}_i + \boldsymbol{K}_{i,c}^T\boldsymbol{e}_{t,k} \leq u_{r,i,k} \leq \bar{u}_i + \boldsymbol{K}_{i,c}^T\boldsymbol{e}_{t,k},\ i = 1, \ldots, n_u\}, \tag{32}$$

where $\boldsymbol{K}_{j,c}$ signifies the jth row of $\boldsymbol{K}_c^T$. The aim is thus to ascertain $\boldsymbol{u}_{r,k}$ in compliance with (32) to ensure $\boldsymbol{u}_k$ meets (6). Given the direct accessibility of $\boldsymbol{e}_{t,k}$ and its forthcoming one-step projection $\boldsymbol{e}_{t,k+1}$ as specified by (14), but the infeasibility of determining $\boldsymbol{e}_{t,k+j}$ for $j > 1$ without knowledge of $\boldsymbol{y}_{k+j}$ and $\hat{\boldsymbol{x}}_{k+j}$, it necessitates resorting to worst-case values. Clearly, $\boldsymbol{e}_{t,k} = \boldsymbol{e}_{r,k} - \boldsymbol{e}_k$ with both $\boldsymbol{e}_{r,k}^T\boldsymbol{P}_c\boldsymbol{e}_{r,k} \leq 1$ and $\bar{\boldsymbol{e}}_k^T\boldsymbol{P}_e\bar{\boldsymbol{e}}_k \leq 1$, leading to $\boldsymbol{e}_{i,r,k} \in \left[-\sqrt{\boldsymbol{P}_{c,i,i}^{-1}}, \sqrt{\boldsymbol{P}_{c,i,i}^{-1}}\right]$ and $\boldsymbol{e}_{i,r,k} \in \left[-\sqrt{\boldsymbol{P}_{e,i,i}^{-1}}, \sqrt{\boldsymbol{P}_{e,i,i}^{-1}}\right]$ for $i = 1, \ldots, n_x$. This enables the definition at discrete time k of an outer-bounding set for $\mathbb{U}r, k+j$, $\mathbb{U}r, k+j \subseteq \bar{\mathbb{U}}r, k+j$, as:

$$\bar{\mathbb{U}}_{r,k+j} = \{u_{r,k+j} : \underline{u}_i + \boldsymbol{K}_{i,c}^T\boldsymbol{d}_{1,k+j} \leq u_{r,i,k} \leq \bar{u}_i + \boldsymbol{K}_{i,c}^T\boldsymbol{d}_{2,k+j}, \quad i = 1, \ldots, n_u\}, \tag{33}$$

and subsequently, the modifications for $\boldsymbol{d}_{1,i,k+j}$ and $\boldsymbol{d}_{2,i,k+j}$ as appropriate.

Following this, since $\boldsymbol{x}_k = \boldsymbol{e}_{r,k} + \boldsymbol{x}_{r,k}$, the inequalities (5) result in the definition of $\mathbb{X}r, k+j$ and its outer-bounding set, $\mathbb{X}r, k+j \subseteq \bar{\mathbb{X}}r, k+j$, outlined as:

$$\bar{\mathbb{X}}_{r,k+j} = \{x_{r,k+j} : \underline{x}_i + \sqrt{\boldsymbol{P}_{c,i,i}^{-1}} \leq x_{i,r,k+j} \leq \leq \bar{x}_i - \sqrt{\boldsymbol{P}_{c,i,i}^{-1}}, \quad i = 1, \ldots, n_x\}. \tag{34}$$

Equipped with the admissible sets for reference input $\boldsymbol{u}_{r,k+j}$ and state $\boldsymbol{x}_{r,k+j}$ as defined in (32) and (34), an algorithm can be devised to pinpoint $\boldsymbol{u}_{r,k}$ that ensures the system's output, as described by (9), effectively tracks the designated reference $\boldsymbol{r}_k$. Herein, the MPC framework is applied [2], [13], following established protocols in the literature. The optimization problem which boils down to

$$J(\boldsymbol{x}_{r,k}, \boldsymbol{r}, \boldsymbol{u}_r, N_p) = \sum_{t=k}^{k+N_p-1} L(\boldsymbol{x}_{r,t}, \boldsymbol{r}_t, \boldsymbol{u}_{r,t}) + V_f(x(k+N_p)), \tag{35}$$

with respect to $\boldsymbol{u}_{r,t,t+N_p-1}$, under the following constraints:

- the reference system dynamics (7)

$$\boldsymbol{x}_{r,t+1} = \boldsymbol{A}(\boldsymbol{p}_k)\boldsymbol{x}_{r,t} + \boldsymbol{B}(\boldsymbol{p}_k)\boldsymbol{u}_{r,t} + \boldsymbol{B}(\boldsymbol{p}_k)\hat{\boldsymbol{f}}_t. \tag{36}$$

- the input and state constraints (33) and (34), $j \in 0, 1, \ldots, N_p - 1$.
- the terminal state constraint $\boldsymbol{x}_{r,t+N_p} \in \mathbb{X}_f$,

is to be solved within the constraints set by system dynamics, input and state limitations, and the finite horizon objective, incorporating the stage cost, terminal penalty, and terminal set definitions.

This on-line operational methodology consists of cyclically executing the steps for state and actuator fault estimation, solving the constrained optimization problem to ascertain the reference state and input, and applying the FTC law to manage the system dynamics effectively, ensuring adherence to the prescribed control objectives and constraints.

V. Illustrative Example

Consider a two-tank system (depicted in Fig 2) to illustrate the effectiveness of the proposed methodology. This system

Fig. 2. A two tank system

is composed of two independent tanks arranged vertically, with one tank positioned above the other. Additionally, it features two pumps: the first pump fills the upper tank with water, while the second pump fills the lower tank. The water is drained from these tanks by gravity. The system's mathematical model can be described in the state-space representation as follows:

$$\boldsymbol{A}_c = \begin{bmatrix} \frac{-K}{2F\sqrt{h_1}} & 0 \\ \frac{K}{2F\sqrt{h_1}} & \frac{-K}{2F\sqrt{h_2}} \end{bmatrix}, \quad \boldsymbol{B}_c = \begin{bmatrix} \frac{1}{F} & 0 \\ 0 & \frac{1}{F} \end{bmatrix}. \tag{37}$$

Having regards the nonlinear behavior of the system as well as its rank, all the matrices shaping the T-S model are given as follows:

$$\boldsymbol{A}_1 = \begin{bmatrix} 0.8397 & 0.0000 \\ -0.0318 & 0.8397 \end{bmatrix}, \boldsymbol{A}_2 = \begin{bmatrix} 0.8397 & 0.0000 \\ -0.0318 & 1.0264 \end{bmatrix},$$
$$\boldsymbol{A}_3 = \begin{bmatrix} 0.8397 & 0.0000 \\ 0.1549 & 0.8397 \end{bmatrix}, \boldsymbol{A}_4 = \begin{bmatrix} 0.8397 & 0.0000 \\ 0.1549 & 1.0264 \end{bmatrix},$$
$$\boldsymbol{A}_5 = \begin{bmatrix} 1.0264 & 0.0000 \\ -0.0318 & 0.8397 \end{bmatrix}, \boldsymbol{A}_6 = \begin{bmatrix} 1.0264 & 0.0000 \\ -0.0318 & 1.0264 \end{bmatrix},$$
$$\boldsymbol{A}_7 = \begin{bmatrix} 1.0264 & 0.0000 \\ 0.1549 & 0.8397 \end{bmatrix}, \boldsymbol{A}_8 = \begin{bmatrix} 1.0264 & 0.0000 \\ 0.1549 & 1.0264 \end{bmatrix},$$
$$\boldsymbol{B} = \begin{bmatrix} 0.2534 & 0.0000 \\ 0.0229 & 0.2534 \end{bmatrix}.$$

It is also important to note that all outputs were measured during the experiments, resulting in $\boldsymbol{C}_c = \boldsymbol{I}_{m \times m}$. The discretization with a sampling time of $T_s = 1[s]$ was set.

To evaluate the effectiveness of the proposed method in terms of fault estimation and fault-tolerant control, a very fault scenario was examined. The specifics of that fault scenario are outlined in Table I. The table clearly shows that

TABLE I
FAULT SCENARIOS PERFORMED DURING THE EXPERIMENT

	pump-1	pump-2
F-Sc	-0.4	-0.6

faults of varying magnitudes were considered. A value of 0 signifies a scenario without faults, whereas -1 represents a complete failure of the actuator. The faults were introduced at a set time of $40[s]$ for the first actuator and $60[s]$ for the second, measured from the start of the experiment. The objective of the control during these tests was to reach and maintain specified water levels in each tank, with the target levels set at $0.4[m]$ for the upper tank and $0.5[m]$ for the lower tank, respectively.

To illustrate the control efficacy, Fig. 3 displays the system's response utilizing the proposed methodology. For comparison, responses involving Fault-Tolerant Control (FTC) based on fault estimation and Model Predictive Control (MPC) are also depicted. The black line represents the actual system response using fault-tolerant control. The green line shows the estimated state of the system provided by the estimator. Denoted by the blue line, this is the reference signal that the system is attempting to track. The red line indicates the system response under model predictive control. The FTC response and its estimate both closely follow the FTC reference, suggesting that the fault-tolerant control method and its estimator are effectively tracking the reference signal. The FTC appears to be slightly closer to

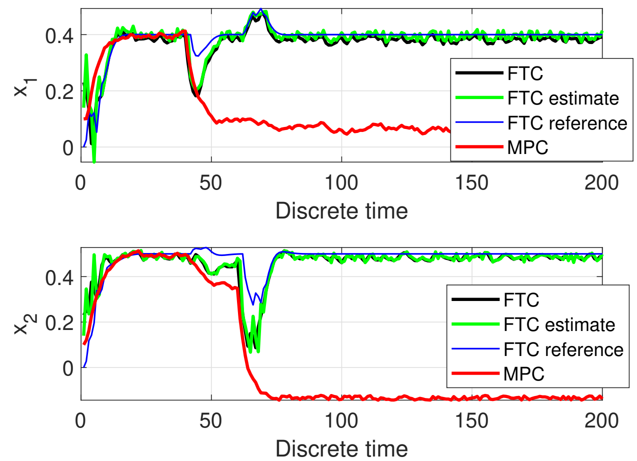

Fig. 3. States of the system for FTC and MPC

the reference than the FTC estimate, which is expected as the estimate is an approximation of the actual state. The MPC control (red line) seems to deviate more significantly from the reference than the FTC method, particularly in the second plot for $\boldsymbol{x}_2$. This suggests that in these scenarios, the FTC method may outperform MPC in terms of following the reference signal closely. There are noticeable drops in both system responses around the time intervals of 50 and 150 discrete time units, which could indicate faults being introduced to the system. The FTC and its estimator recover and return to following the reference signal shortly after these faults, demonstrating resilience and effective fault-tolerant behavior. The FTC estimate closely tracks the actual FTC response, which indicates that the estimator within the FTC is performing well. It seems to provide an accurate estimation of the system's state even in the presence of faults. Both $\boldsymbol{x}_1$ and $\boldsymbol{x}_2$ show similar patterns in response to the controls, suggesting that the system's behavior is consistent across its different states or outputs. Such a FTC control quality stands for a result of good fault estimation quality. Fig. 4 presents real actuator fault (given by red line)

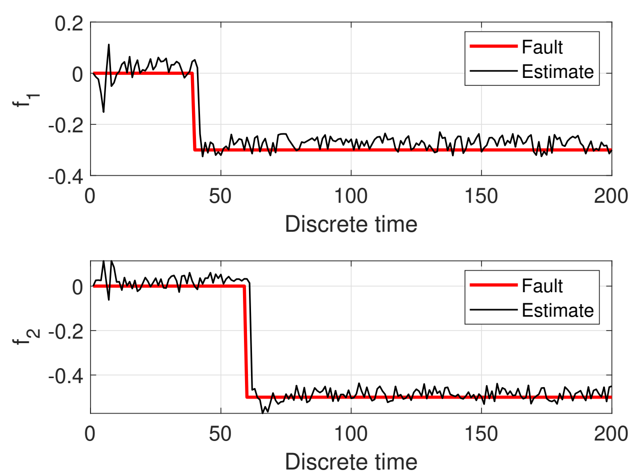

Fig. 4. Actuator fault and their estimates

occurred in the system along with their estimates (given by black line). The estimates closely match the actual faults for both actuators, indicating a high precision of the estimation algorithm in diagnosing faults. The fault estimates appear to react quickly to changes. In both cases, we can see the estimates' spikes occurring shortly after the faults present themselves, suggesting that the estimation system can detect the occurrence of a fault rapidly. According to fault scenario, in both cases the faults are shown as sudden changes in value occurring in 40-th and 60-th seconds from start. The faults remain at a constant level, indicating that these are step faults, where the fault introduced into the system maintains a consistent level post-occurrence. In the case of the first pump, it is shown slight fluctuations in fault estimation before the fault occurs, which could represent measurement noise or minor disturbances. After the fault occurs, however, the estimate remains stable and closely tracks the fault without visible overshoots. The other important aspect during the

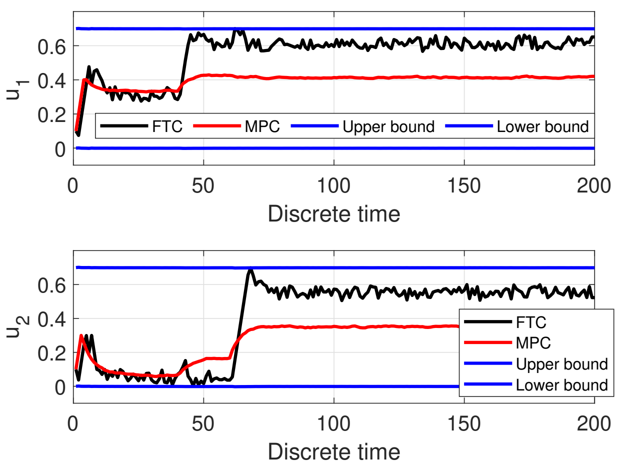

Fig. 5. Control signals of the compared algorithms

experiment was the analysis of the control signal performed with the proposed approach along with MPC ones to which FTC was compared. In the Fig. 5 the mentioned control signals are presented for the control scenarios. It is evident that the proposed approach is capable of modifying the control law based on the occurrence of faults in order to compensate for the effects of the faults, in contrast to MPC, which was not able to steer the system in such a way as to reach and maintain tracking of the reference signal.

The figures presented clearly demonstrate that the proposed strategy effectively addresses faults, including those resulting in up to a 60% reduction in efficiency.

VI. Conclusions

The primary aim of this paper is to introduce an innovative integrated fault-tolerant control methodology for constrained non-linear systems that are subject to bounded external disturbances. This method is implemented using the quadratic boundedness approach, enabling the formulation of necessary and sufficient conditions for the integration of fault estimation and fault-tolerant control. The strategy devised is based on output feedback, designed to follow the desired reference trajectory while accounting for faults, disturbances, and constraints on both state and input. The achieved results clearly indicate the superiority of the proposed approach over the MPC one being compared.

References

[1] A. Alessandri, M. Baglietto, and G. Battistelli. Design of state estimators for uncertain linear systems using quadratic boundedness. *Automatica*, 42:497–502, 2006.

[2] E.F. Camacho and C. Bordons. *Model predictive controllers*. Springer, 2007.

[3] S. de Oca, V. Puig, M. Witczak, and L Dziekan. Fault-tolerant control strategy for actuator faults using lpv techniques: Application to a two degree of freedom helicopter. *International Journal of Applied Mathematics and Computer Science*, 22(1):161–171, 2012.

[4] M.-H. Do, D. Koenig, and D. Theilliol. Robust h∞ proportional-integral observer-based controller for uncertain lpv system. *Journal of the Franklin Institute*, 357(4):2099–2130, 2020.

[5] Paulin Kantue and Jimoh O Pedro. Integrated fault-tolerant control of a quadcopter uav with incipient actuator faults. *International Journal of Applied Mathematics and Computer Science*, 32(4), 2022.

[6] Boutrous Khoury, Fatiha Nejjari Akhi-Elarab, and Vicenç Puig Cayuela. Reliability-aware zonotopic tube-based model predictive control of a drinking water network. *International journal of applied mathematics and computer science*, 32(2):197–211, 2022.

[7] Norbert Kukurowski, Marcin Mrugalski, Marcin Pazera, and Marcin Witczak. Fault-tolerant tracking control for a non-linear twin-rotor system under ellipsoidal bounding. *International Journal of Applied Mathematics and Computer Science*, 32(2):171–183, 2022.

[8] Ayyoub Ait Ladel, Abdellah Benzaouia, Rachid Outbib, and Mustapha Ouladsine. Integrated state/fault estimation and fault-tolerant control design for switched t–s fuzzy systems with sensor and actuator faults. *IEEE Transactions on Fuzzy Systems*, 30(8):3211–3223, 2021.

[9] J. Lan and R. Patton. An iterative strategy for robust integration of fault estimation and fault-tolerant control. *Automatica*, 145:110556, 2022.

[10] J. Lan and R.J. Patton. Integrated design of fault-tolerant control for nonlinear systems based on fault estimation and t–s fuzzy modeling. *IEEE Transactions on Fuzzy Systems*, 25(5):1141–1154, 2016.

[11] J. Lan and R.J. Patton. A new strategy for integration of fault estimation within fault-tolerant control. *Automatica*, 69:48–59, 2016.

[12] J. Lan and R.J. Patton. *Robust integration of model-based fault estimation and fault-tolerant control*. Springer, 2021.

[13] Lalo Magni, Davide Martino Raimondo, and Riccardo Scattolini. Regional input-to-state stability for nonlinear model predictive control. *IEEE Transactions on automatic control*, 51(9):1548–1553, 2006.

[14] Marcin Mrugalski. *Advanced Neural Network-based Computational Schemes for Robust Fault Diagnosis*. Springer-Verlag, Berlin-Heidelberg, 2014.

[15] Junbo Tan, Huailiang Zheng, Deshan Meng, Xueqian Wang, and Bin Liang. Active input design for simultaneous fault estimation and fault-tolerant control of lpv systems. *Automatica*, 151:110903, 2023.

[16] Pan Tang, Fubiao Zhang, Jianchuan Ye, and Defu Lin. An integral tsmc-based adaptive fault-tolerant control for quadrotor with external disturbances and parametric uncertainties. *Aerospace Science and Technology*, 109:106415, 2021.

[17] M. Witczak, L. Dziekan, V. Puig, and J. Korbicz. Design of a fault-tolerant control scheme for takagi-sugeno fuzzy systems. In *2008 16th Mediterranean Conference on Control and Automation*, pages 280–285. IEEE, 2008.

[18] M. Witczak, V. Puig, and S. de Oca. A fault-tolerant control strategy for non-linear discrete-time systems: application to the twin-rotor system. *International Journal of Control*, 86(10):1788–1799, 2013.

[19] M. Witczak, L. Seybold, E. Bulach, and N. Maucher. *Modern IoT Onboarding Platforms for Advanced Applications. A Practitioner's Guide to KIS.ME*. Springer-Verlag, Berlin-Heidelberg, 2023.

[20] Yanzheng Zhu and Wei Xing Zheng. An integrated design approach for fault-tolerant control of switched lpv systems with actuator faults. *IEEE Transactions on Systems, Man, and Cybernetics: Systems*, 53(2):908–921, 2022.